View metadata, citation and similar papers at core.ac.uk

brought to you by CORE

provided by Bangor University Research Portal

PRIFYSGOL BANGOR / BANGOR UNIVERSITY

The effect of mirabilite precipitation on the absolute and practical salinities of sea ice brines

Butler, Benjamin; Papadimitriou, Efstathios; Kennedy, Hilary

Marine Chemistry

DOI:
10.1016/j.marchem.2016.06.003

Published: 20/08/2016

Peer reviewed version

Cyswllt i'r cyhoeddiad / Link to publication

Dyfyniad o'r fersiwn a gyhoeddwyd / Citation for published version (APA):
Butler, B., Papadimitriou, E., & Kennedy, H. (2016). The effect of mirabilite precipitation on the absolute and practical salinities of sea ice brines. *Marine Chemistry*, *184*(August), 21-31. https://doi.org/10.1016/j.marchem.2016.06.003

Hawliau Cyffredinol / General rights
Copyright and moral rights for the publications made accessible in the public portal are retained by the authors and/or other copyright owners and it is a condition of accessing publications that users recognise and abide by the legal requirements associated with these rights.

• Users may download and print one copy of any publication from the public portal for the purpose of private study or research.
• You may not further distribute the material or use it for any profit-making activity or commercial gain
• You may freely distribute the URL identifying the publication in the public portal ?

Take down policy
If you believe that this document breaches copyright please contact us providing details, and we will remove access to the work immediately and investigate your claim.

09. Oct. 2020

The effect of mirabilite precipitation on the absolute and practical salinities of sea ice brines

Benjamin Miles Butler[a], Stathys Papadimitriou[a], Hilary Kennedy[a]

[a]*School of Ocean Sciences, Bangor University, Menai Bridge, Anglesey, LL59 5AB, UK*

Abstract

The sea ice cover of high latitude oceans contains concentrated brines which are the site of *in-situ* chemical and biological reactions. The brines become supersaturated with respect to mirabilite ($Na_2SO_4 \cdot 10H_2O$) below -6.4 °C, and the associated removal of Na^+ and SO_4^{2-} from the brine results in considerable non-conservative changes to its composition. The changes are reflected in the brine salinity, which is a fundamental physico-chemical parameter in the sea ice brine system. Here, measurements of electrical conductivity and brine composition in synthetic sea ice brines between -1.8 and -20.6 °C, obtained during a comprehensive investigation of the brine-mirabilite equilibrium at below-zero temperatures reported elsewhere, are combined with modelled estimates to assess the behaviour of the absolute (S_A) and practical (S_P) salinities of sea ice brines. Results display substantial divergence of S_P from S_A below -6.4 °C, reaching a 7.2 % difference at -22.8 °C. This is shown to create inaccuracies when S_P is assumed to be equivalent to S_A, firstly by misrepresenting the conditions inhabited by sea ice biota, whilst also creating errors in the calculation of physical sea ice parameters. Our measured and modelled data are used to refine the $S_A - T$ relationship for sea ice brines, implicit of mirabilite precipitation, which is crucial in estimat-

ing brine properties in absence of salinity data. Furthermore, because S_P is the parameter measured in field studies, we provide an $S_P - T$ relationship for sea ice brines to -22.8 °C, which aids in explaining the trends observed in available $S_P - T$ data from sea ice brines in the Southern Ocean, demonstrating the importance of the mirabilite-brine equilibrium in natural sea ice. Finally, we initiate the development of a conversion factor for the estimation of S_A from S_P measurement in sea ice brines, and produce an equation that can calculate S_A from modelled brine density. This work ultimately highlights careful consideration of salinity concepts when applied to the sea ice system.

Keywords: Mirabilite, Sea ice, Salinity, FREZCHEM

1. Introduction

The Na−K−Mg−Ca−Cl−SO_4−H_2O system describes 99.4 % of the major dissolved ions in Standard Seawater by weight (Millero et al., 2008), and these ions have long been known to display constant ratios to one another throughout the world ocean (Forchhammer, 1865; Dittmar et al., 1873). This conservative behaviour gave rise to the concept of salinity, which was originally defined as a measure of the mass of dissolved salts per unit mass of seawater and is now termed absolute salinity (S_A) (Lewis, 1980). Accurate and rapid determination of salinity is paramount in the calculation of seawater density (Millero et al., 2008; Pawlowicz, 2015), therefore, since the advent of salinity as a concept, the method of its measurement has evolved to its present form of determination from measurement of electrical conductivity (Fofonoff, 1985; Lewis, 1980). The combined contribution of charged

dissolved species to the total electrical conductivity of a solution is a conservative property and its measurement is converted to 'practical' salinity (S_P) by the Practical Salinity Scale 1978 (PSS-78). According to the PSS-78 definition (Perkin and Lewis, 1980), the S_P of a solution is derived from the ratio (R_{15}) of the total electrical conductivity of the solution to that of a solution of potassium chloride (KCl) in pure water with a KCl mass fraction of 32.4356 g when both solutions are at 15 °C on the IPTS-68 scale, and zero gauge pressure (Fofonoff, 1985; Lewis, 1980; Millero et al., 2008). Practical salinity is dimensionless, and when $R_{15} = 1$, $S_P = 35$. The reproducibility of conductivity measurements is good enough for deep sea research where S_P accuracies within ±0.006 (King et al., 2001) are required, and is now the dominant method for salinity measurement in both oceanography at sea and in the laboratory. Measurement of S_P also allows for precise calculation of S_A based on the most recent accurate chemical analysis defining $S_A = 35.16504$ g $kg^{-1}_{solution}$ in Standard Seawater with $S_P = 35$ (Millero et al., 2008), with $S_A/S_P = 1.004715 \pm 0.0005$ (Jackett et al., 2006; Pawlowicz, 2012; Millero et al., 2008; Millero and Huang, 2009). This relationship is valid for practical salinities between 2 and 42, which is the working salinity range of the PSS-78 (Lewis, 1980; Pawlowicz, 2012).

The electrical conductivity of a solution is a function of its temperature, the total amount of charged species dissolved in it, and their inter-ionic ratios (Weeks, 2010). Deviations from the constant stoichiometric ratios of Standard Seawater (table 1) will occur as a result of any process that leads to non-conservative behaviour of the major ions, with the formation of seawater-derived brines in evaporative or cryospheric environments providing

apt examples (McCaffrey et al., 1987; Marion et al., 1999; Grasby et al., 2013; Butler et al., 2016). Amongst the best studied cryospheric environments on Earth is the sea ice cover of high latitude oceans, which extends over approximately 20 million km^2 seasonally (Dieckmann and Hellmer, 2010), covering $\sim$5 % of the Earths surface. Sea ice undergoes large changes in temperature, chemical composition, and structure throughout its seasonal cycle (Gleitz et al., 1995), which are reflected in the labyrinth of inclusions within the ice that contain rejected liquid brine at local ice-brine (thermal) equilibrium (Weeks and Ackley, 1986; Petrich and Eicken, 2010; Light et al., 2003; Golden et al., 2007). At the low temperature (-1.8 to ~ -35 °C; Miller et al., 2011) and hypersaline conditions (up to $\sim$220 g $kg^{-1}_{solution}$; Ewert and Deming, 2013) of sea ice brines, a suite of dissolved salts reach saturation with respect to their, typically hydrated, solid phases, which precipitate. The current understanding of solid-solution equilibria in sea ice states the following sequence of precipitates from sea ice brine as it cools to its eutectic: ikaite ($CaCO_3 \cdot 6H_2O$) at temperatures less than -2 °C (depending on brine pCO_2; Papadimitriou et al., 2013), mirabilite ($Na_2SO_4 \cdot 10H_2O$) at -6.4 °C (Butler et al., 2016), hydrohalite ($NaCl \cdot 2H_2O$) at -22.9 °C (Marion et al., 1999; Butler and Kennedy, 2015), sylvite (KCl) at -33 °C, and $MgCl_2 \cdot 12H_2O$ at -36.2 °C (Gitterman, 1937; Nelson and Thompson, 1954). In addition to this sequence, gypsum ($CaSO_4 \cdot 2H_2O$) may also precipitate (Gitterman, 1937; Marion et al., 1999), though estimates for the temperature region of its precipitation are conflicting, and range from -3 °C (Geilfus et al., 2013) to -22.2 °C (Marion et al., 1999).

Salt precipitation in sea ice can result in substantial non-conservative

changes in the ionic composition of the brine; recent measurements indicate that mirabilite precipitation results in a reduction of the total concentrations of Na^+ and SO_4^{2-} by up to 13 % and 92 %, respectively, by -20.6 °C (Butler et al., 2016). The changes are particularly significant given that these ions contribute approximately 38 % to S_A (table 1) and 30 % to the total electrical conductivity of the solution.

Table 1: A comparison of the compositions of Simplified (DOE, 1994) and Standard (Millero et al., 2008) Seawater. The remaining ions in Standard Seawater that are not tabulated include: Sr^{2+}, HCO_3^-, Br^-, CO_3^{2-}, $B(OH)_4^-$, F^-, OH^-, $B(OH)_3$ and CO_2.

	$S_P = 35$	
	Simplified seawater	Standard Seawater
Solute	g kg_{sol}^{-1}	
Na^+	10.7848	10.7815
K^+	0.3992	0.3991
Mg^{2+}	1.2840	1.2837
Ca^{2+}	0.4152	0.4121
Cl^-	19.4715	19.3527
SO_4^{2-}	2.7128	2.7124
H_2O	964.93	964.83
Remaining ions	N/A	0.2285

Salt precipitation in sea ice is confined to the brine inclusions that permeate its structure, ranging in diameter from 10 μm to 10 mm depending on the ice temperature (Light et al., 2003). The physical and chemical properties of the brine define the conditions inhabited by the sympagic (within

ice) community, which is comprised of bacteria, microalgae, viruses, fungi, protozoans, and small metazoans (Horner et al., 1992; Thomas and Dieckmann, 2002; Ewert and Deming, 2013). Microscopic biota potentially covers between 6 and 41 % of the brine channel surface area at −2 °C (Krembs et al., 2000), while salt precipitates at colder temperatures may provide additional solid surfaces with which microorganisms can interact (Ewert and Deming, 2013). The salinity of the brine within the inclusions is temperature-dependent (Assur, 1960) and represents one of the major constraints on resident sea ice organisms because it affects the function of proteins and the surrounding osmotic conditions (Ewert and Deming, 2013). Brine salinities in sea ice extend from diluted seawater during ice melt with salinities <30 g $kg^{-1}_{solution}$, to salinities exceeding ∼220 g $kg^{-1}_{solution}$ during winter months when the ice is at its coldest. For this reason, an accurate representation of brine salinity is required for determining the physico-chemical conditions of the internal sea ice habitat (Thomas et al., 2010; Ewert and Deming, 2013).

Sea ice salinity is most often measured as a bulk property, determined as S_P in melted sea ice samples. Measurements of bulk sea ice S_P are then used to estimate the physical parameters of the ice pack, such as brine volume fraction and porosity (Cox and Weeks, 1988; Gleitz et al., 1995; Petrich and Eicken, 2010). In such instances, the salinity of the internal brines can be estimated as S_A from the ice temperature via available liquidus equations (Assur, 1960; Cox and Weeks, 1986; Notz and Worster, 2009), assuming local ice-brine equilibrium, i.e., $T_{ice} = T_{fr}$, where T_{fr} = the freezing point of internal sea ice brine. These equations describe ice, water and salt mass balance as a function of temperature and are based on dissolved salt analysis

provided in the seminal work on seawater freezing by Nelson and Thompson (1954). The accuracy of the original measurements, with respect to mirabilite precipitation in particular, has recently been evaluated from a comprehensive assessment of mirabilite solubility in equilibrium sea ice brines (Butler et al., 2016). Discrepancies include indications for mirabilite-brine disequilibrium in the freezing experiments of Nelson and Thompson, and a warmer onset temperature of mirabilite precipitation (-6.4 °C) than previously thought (-8.2 °C). These discrepancies will be reflected in the liquidus ($S_\mathrm{A} - T_\mathrm{fr}$) equations for the ice-brine equilibrium (Assur, 1960; Cox and Weeks, 1986; Notz and Worster, 2009). In light of these recent developments, there is scope for refinement of the $S_\mathrm{A} - T_\mathrm{fr}$ relationship. In addition, while the liquidus equation in sea ice yields the S_A of the internal brines from ice temperature measurements, S_P is the property that is directly measured in sea ice brines as afforded by the available oceanographic instruments and protocols. Such brine samples are typically obtained by centrifugation or by drilling bore holes through the surface to varying depth in the ice (sackhole brines), and represent conditions that extend well into the temperature-salinity region of salt precipitation (Krembs et al., 2000; Papadimitriou et al., 2004; Munro et al., 2010; Norman et al., 2011; Garrison et al., 2003). Universally in sea ice research, the difference between brine S_A (from the liquidus equation) and S_P (as typically measured directly) is assumed to be insignificant or is ignored (Munro et al., 2010; Garrison et al., 2003; Norman et al., 2011). Therefore, there is also a pressing need for rigorous evaluation of the relevance of S_P measurements and of the S_A and S_P relationship in non-conservative sea ice brines.

Here, we examine the effect of salt precipitation on the practical and absolute salinities of synthetic sea ice brines at thermal equilibrium between -1.8 to -20.6 °C using laboratory measurements of S_A and S_P during an extensive investigation of the mirabilite-brine equilibrium at below-zero temperatures reported in Butler et al. (2016). In addition, we use the FREZCHEM thermodynamic code and equations for the electrical conductivity of individual ions (McCleskey et al., 2012) to model S_A and S_P in our experimental conditions. The FREZCHEM code has been developed for the study of cold aqueous geochemistry (Marion and Kargel, 2008) and has been used in the investigation of physical-chemical processes in sea ice (Marion et al., 1999; Grasby et al., 2013; Geilfus et al., 2013; Papadimitriou et al., 2013), and is particularly accurate in computing ice-brine-mirabilite equilibria in sea ice brines (Butler et al., 2016). Lastly, measured and modelled data are compared to $S_P - T$ data of natural sea ice brines from the Southern Ocean (Gleitz et al., 1995; Norman et al., 2011). Together the data are used; to assess and refine the existing $S_A - T_{fr}$ relationship compared to several empirical liquidus equations currently in use; to define a novel $S_P - T_{fr}$ relationship for sea ice brines implicit of mirabilite precipitation; develop a conversion factor that can account for the changing S_A to S_P ratio in sea ice brines affected by mirabilite precipitation; and to produce an empirical equation for the estimation of S_A from sea ice brine density.

2. Methods

2.1. Closed bottle incubations

A detailed account of the experimental protocol carried out for this investigation is provided in Butler et al. (2016). Synthetic brines were prepared with the method of Kester et al. (1967) according to the composition of simplified seawater (DOE, 1994) with respect to NaCl, KCl, $MgCl_2$, $CaCl_2$, and Na_2SO_4 (table 1). Synthetic brines were used in order to simplify the protocol for the determination of S_A, requiring the measurement of 6 ions per sample compared to the 14 per sample that would be required for natural solutions (table 1). The brines were incubated in triplicate in screw-capped (Teflon-lined) borosilicate media bottles at 2 °C below their estimated freezing point according to the salinity/freezing-point relationship for seawater in Millero and Leung (1976). The experimental temperatures ranged from −1.8 to −20.6 °C, with mirabilite being the only salt precipitate detected (by brine analysis and synchrotron X-ray powder diffraction), forming at temperatures $\leqslant$−6.4 °C (Butler et al., 2016).

2.2. Measurement of absolute and practical salinities

The absolute salinity (S_A^{meas}) of the experimental solutions was obtained by mass balance from measurement of the total ion concentrations in solution (Na^+, K^+, Mg^{2+}, Ca^{2+}, Cl^-, and SO_4^{2-}). The Na^+ and K^+ concentrations were determined by ion chromatography on a Dionex Ion Exchange Chromatograph ICS 2100. The Mg^{2+} and Ca^{2+} concentrations were determined by potentiometric titration as described by Papadimitriou et al. (2013). The Cl^- concentration was determined by gravimetric Mohr titration with 0.3 M

$AgNO_3$ standardized against NaCl purified by recrystallization. The SO_4^{2-} concentration was determined by precipitation as $BaSO_4$ in EDTA followed by gravimetric titration with $MgCl_2$ (Howarth, 1978). Repeat measurements of local seawater collected from the Menai Strait (53.1806°N, 4.2333°W) were used as an internal standard relative to the composition of Standard Seawater (Millero et al., 2008). This comparison provided an estimate of accuracy of the measurements, which was 0.33 % for Na^+, −0.97 % for K^+, −0.36 % for Mg^{2+}, −0.39 % for Ca^{2+}, 0.48 % for Cl^-, and 0.35 % for SO_4^{2-}. The measured solution concentrations (mol kg_{sol}^{-1}) were converted to g kg_{sol}^{-1} using the atomic masses provided by the International Union of Pure and Applied Chemistry (IUPAC). The S_A^{meas} (g kg_{sol}^{-1}) was then calculated as follows:

$$S_A = \sum_{i=1}^{n} c_i MW_i \tag{1}$$

where the i^{th} of n constituents has a concentration of c_i (mol kg_{sol}^{-1}) and molecular mass MW_i (g mol^{-1}) (Pawlowicz, 2012). The combined analytical and experimental errors yield an estimated accuracy of 0.22 % for S_A^{meas}, equivalent to $S_A^{meas} = 35.07$ at $S_A = 35.00$ g kg_{sol}^{-1}. Note that our absolute salinity S_A is actually the Solution Absolute Salinity S_A^{soln} of the new Thermodynamic Equation of Seawater - 2010 (IOC et al., 2010).

At present, there is no standard way of measuring practical salinities outside of the range specified in PSS-78, and in high salinity media, such as sea ice brines, samples are analysed by warming to laboratory temperature followed by gravimetric dilution with pure water to values within the measurable range of PSS-78 (Pawlowicz, 2012; Norman et al., 2011; Gleitz et al., 1995; Papadimitriou et al., 2007). Here, practical salinity was mea-

sured ($S_{\mathrm{P}}^{\mathrm{meas}}$) using a portable conductivity meter (WTW Cond 3110) with a WTW Tetracon 325 probe at laboratory temperature ($20 - 26$ °C) following gravimetric dilution with distilled water to a target S_{P} of 35. The electrical conductivity (k) and, hence, the values of $S_{\mathrm{P}}^{\mathrm{meas}}$ given by this instrument are automatically corrected to 25 °C (k_{25}). The conductivity meter was calibrated in the $k_{25} = 10 - 95$ mS kg cm^{-1} mol^{-1} conductivity range, covering an S_{P} range of $10 - 70$, against a Guildline AUTOSAL oceanographic salinometer (instrument accuracy in $S_{\mathrm{P}} = \pm 0.002$), itself calibrated with IAPSO Reference Seawater ($S_{\mathrm{P}} = 35$). For this calibration we used local seawater ($S_{\mathrm{P}} = 33 - 34$, assuming ionic ratios equivalent to Standard Seawater) and a range of diluted (with ultrapure MilliQ water) and concentrated (by freezing; Butler et al., 2016) solutions prepared from it. The S_{P} measured by this instrument can be described as a second order polynomial function of k_{25} ($R^2 = 0.9998$, $n = 336$, $p =< 0.001$), where

$$S_{\mathrm{P}} = -0.039056 + 0.572499 k_{25} + 0.001589 k_{25}^2 \tag{2}$$

with an estimated standard error of ± 0.14. Lastly, the S_{P} measured by the conductivity meter was multiplied by the dilution factor to obtain $S_{\mathrm{P}}^{\mathrm{meas}}$.

2.3. Prediction of absolute salinity with FREZCHEM

Using the chemical composition of our synthetic brines and enabling only the formation of ice and mirabilite in its solid phase database, the thermodynamic code FREZCHEM (Marion and Kargel, 2008; Marion et al., 2010) was used to model the absolute salinity ($S_{\mathrm{A}}^{\mathrm{mod}}$) of equilibrium sea ice brines. The code was run in 0.1 °C steps between -1.8 and -22.8 °C, and ion concentrations from the output were retrieved at each temperature. The temperature

minimum of the model run is beyond that covered by the laboratory experiments (−20.6 °C) and covers the full temperature range in which mirabilite is the major salt precipitate affecting brine composition in sea ice (Marion et al., 1999; Butler and Kennedy, 2015). In order to calculate $S_{\mathrm{A}}^{\mathrm{mod}}$ using equation 1, the molal (mol $\mathrm{kg}_{\mathrm{H_2O}}^{-1}$) concentrations of the code output were converted to mol $\mathrm{kg}_{\mathrm{sol}}^{-1}$ by

$$\text{mol kg}_{\mathrm{sol}}^{-1} = m \left(\frac{1000}{1000 + \sum_i m_i MW_i} \right), \tag{3}$$

where m_i and MW_i are the molality and molecular mass (g mol^{-1}) of the i^{th} ion in solution, respectively (Marion and Kargel, 2008).

The FREZCHEM code is based on the specific ion interaction model of electrolyte theory as formalized by Pitzer (1973). The Pitzer formalism has been found to account fully for ion-ion interactions except for those which exhibit large ion pair formation constants (He and Morse, 1993). For the synthetic brine compositions that were modelled, FREZCHEM explicitly computed the concentrations of $\mathrm{HSO_4^-}$ and $\mathrm{MgOH^+}$ in addition to the unpaired major ions. Concentrations did not exceed 10^{-6} mol $\mathrm{kg}_{\mathrm{sol}}^{-1}$ for $\mathrm{MgOH^+}$ and 10^{-9} mol $\mathrm{kg}_{\mathrm{sol}}^{-1}$ for $\mathrm{HSO_4^-}$ throughout the conditions of this study, rendering their contribution to $S_{\mathrm{A}}^{\mathrm{mod}}$ negligible.

2.4. Modelling practical salinity with ionic molal conductivities

Because our $S_{\mathrm{P}}^{\mathrm{meas}}$ is based on the total electrical conductivity measured in the synthetic brines as k_{25}, the same property was modelled ($S_{\mathrm{P}}^{\mathrm{mod}}$) using equations from McCleskey et al. (2012). The $S_{\mathrm{P}}^{\mathrm{mod}}$ was calculated for the same chemical composition as the brines from the FREZCHEM modelling,

whilst ensuring that the conductivity calculations were carried out within their specified ionic range (McCleskey et al., 2012). The contribution of HSO_4^- and $MgOH^+$ to total electrical conductivity cannot be calculated using these equations, and again were considered negligible on account of their very low concentrations. The chemical composition of the brines extracted from the FREZCHEM model were normalised to an ionic strength of 0.72 mol $kg_{H_2O}^{-1}$ by the required dilution factor using a solver routine in Microsoft Excel. This dilution step was employed in order to replicate our experimental procedures. The electrical conductivity of each ion i in the solution at 25 °C was calculated by

$$k_{25,i} = \lambda_i m_i \tag{4}$$

where λ_i is the ionic molal conductivity and m_i is the ion molality. The λ_i is calculated as a function of ionic strength (I, molal) and temperature T (°C) by

$$\lambda_i = \lambda^\circ(T) - \frac{A(T)I^{0.5}}{1 + BI^{0.5}} \tag{5}$$

where B is an empirical constant, while λ° and A are functions of temperature described by the equations given in table 2. The ionic strength was calculated using

$$I = 0.5 \sum m_i z_i^2 \tag{6}$$

where z_i is the charge of the i^{th} ion.

The ionic molal conductivities of each ion calculated from equations 4 to 6 were summed to give the total electrical conductivity of the solution at 25 °C (k_{25}). Solution conductivities (mS kg cm^{-1} mol^{-1}) were then converted to S_P according to equation 2, and were multiplied by the dilution factor to attain the undiluted S_P^{mod} of the brine.

Table 2: Equations and constants from McCleskey et al. (2012) used for calculating λ°, A and B for use in equation 5, where T is temperature (°C).

Ion	λ°	A	B
Na^+	$0.003763T^2 + 0.877T + 26.23$	$0.00027T^2 + 1.1410T + 32.07$	1.7
K^+	$0.003046T^2 + 1.261T + 40.70$	$0.00535T^2 + 0.9316T + 22.59$	1.5
Mg^{2+}	$0.010680T^2 + 1.695T + 57.16$	$0.02453T^2 + 1.9150T + 80.50$	2.1
Ca^{2+}	$0.009645T^2 + 1.984T + 62.28$	$0.03174T^2 + 2.3340T + 132.3$	2.8
Cl^-	$0.003817T^2 + 1.337T + 40.99$	$0.00613T^2 + 0.9469T + 22.01$	1.5
SO_4^{2-}	$0.010370T^2 + 2.838T + 82.37$	$0.03324T^2 + 5.8890T + 193.5$	2.6

2.5. Comparison with natural sea ice brine salinities

Our measured and modelled practical and absolute salinities were compared to available sea ice brine salinity data from Gleitz et al. (1995) and Norman et al. (2011). The two studies contain measurements of S_P for sea ice brines that were extracted through drainage into sack-holes. The field dataset spans a brine temperature range from -1.3 to -12.4 °C, with S_P ranging from 29 to 179. All samples were taken from the seasonal ice zone of the Southern Ocean between 1991 and 2007.

3. Results

Both $S_\mathrm{A}^\mathrm{meas}$ and $S_\mathrm{P}^\mathrm{meas}$ increase at nearly identical rates down to -6.4 °C as increasing quantities of pure water are removed as ice to maintain thermal equilibrium (figure 1). In these experimental brines with a conservative composition, $S_\mathrm{A}^\mathrm{meas}/S_\mathrm{P}^\mathrm{meas} = 0.9995 \pm 0.0035$, which is 0.52 % lower than the value of 1.004715 ± 0.0005 in Standard Seawater (Millero et al., 2008; Jack-

ett et al., 2006). This difference is not significant ($p > 0.05$ as tested with a two-tailed t-test with unequal variance), and we attribute it to the use of simplified synthetic seawater composed of 6 major ions (table 1). Below -6.4 °C, $S_{\mathrm{P}}^{\mathrm{meas}}$ increases at a greater rate than $S_{\mathrm{A}}^{\mathrm{meas}}$, coincident with the redistribution of ions consequent of mirabilite precipitation. By -20.6 °C, $S_{\mathrm{P}}^{\mathrm{meas}}$ is 5.7 % higher than $S_{\mathrm{A}}^{\mathrm{meas}}$, which results in $S_{\mathrm{A}}^{\mathrm{meas}}/S_{\mathrm{P}}^{\mathrm{meas}}$ reducing from 0.9995 to 0.9458.

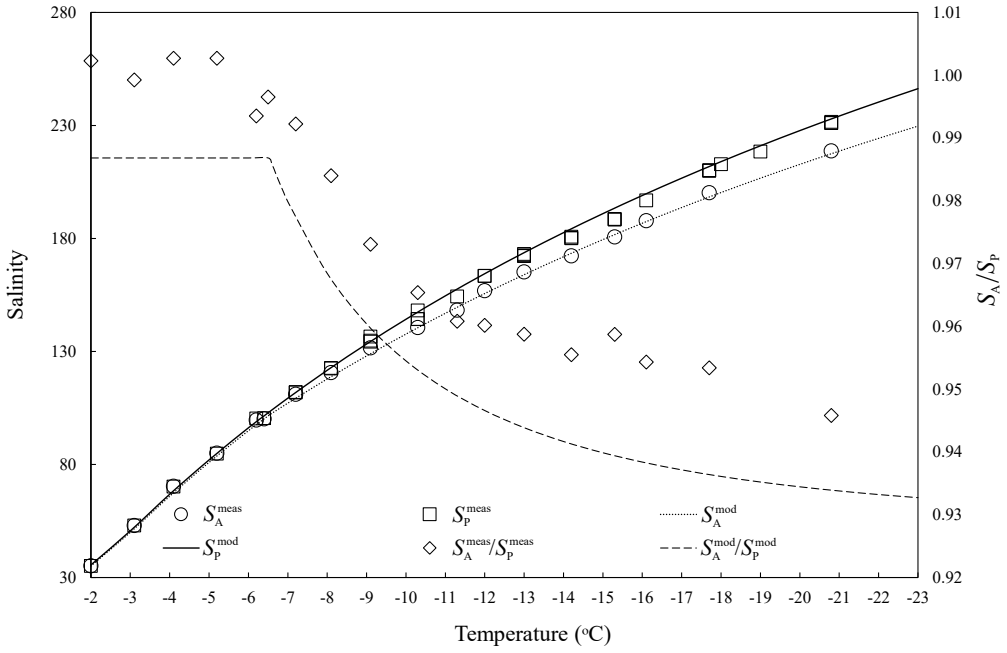

Figure 1: Measured and modelled S_{A} and S_{P} of equilibrium sea ice brines between -1.8 and -22.8 °C, and the associated $S_{\mathrm{A}}/S_{\mathrm{P}}$. The error of the measurements is within the diameter of the symbols.

Measured and modelled data displayed good agreement (figure 1). The average difference between $S_{\mathrm{A}}^{\mathrm{mod}}$ and $S_{\mathrm{A}}^{\mathrm{meas}}$ was 0.89 ± 1.30 %, while that

between $S_{\mathrm{P}}^{\mathrm{mod}}$ and $S_{\mathrm{P}}^{\mathrm{meas}}$ was -0.62 ± 1.36 %, resulting in $S_{\mathrm{A}}^{\mathrm{mod}}/S_{\mathrm{P}}^{\mathrm{mod}}$ being consistently lower than that derived from our measurements by 0.014 ± 0.003. Modelled brines at temperatures above -6.4 °C display an $S_{\mathrm{A}}^{\mathrm{mod}}/S_{\mathrm{P}}^{\mathrm{mod}} = 0.9868$, which reduces to 0.9327 at -22.8 °C when $S_{\mathrm{P}}^{\mathrm{mod}}$ is 7.4 % higher than $S_{\mathrm{A}}^{\mathrm{mod}}$.

Whilst the $S_{\mathrm{P}}^{\mathrm{mod}}$ has inherent inaccuracies (McCleskey et al., 2012), its agreement with the measurements allows its use as a means to assess the changes in the relative contribution of each major ion to the total electrical conductivity of the brines and, hence, S_{P}. A likewise evaluation can be done with respect to S_{A} using $S_{\mathrm{A}}^{\mathrm{mod}}$ (table 3). The decrease in $S_{\mathrm{A}}^{\mathrm{mod}}/S_{\mathrm{P}}^{\mathrm{mod}}$ at temperatures below -6.4 °C (figure 1) is due to compositional changes in the brine relating to the removal of Na^+ and SO_4^{2-} from solution to mirabilite, as well as water in the mirabilite hydration water molecules. The largest decrease in percent contribution to solution conductivity and, hence, $S_{\mathrm{P}}^{\mathrm{mod}}$, is that of SO_4^{2-} during its removal from solution to mirabilite (table 3). The change in percent contribution of Na^+ during the same process is less pronounced because of its 16.6 times larger background concentration (Millero et al., 2008). As a result, the contribution of the remaining ions to the electrical conductivity and $S_{\mathrm{P}}^{\mathrm{mod}}$ increases accordingly. For all ions other than Na^+, the change in percent contribution to $S_{\mathrm{A}}^{\mathrm{mod}}$ is greater than that to $S_{\mathrm{P}}^{\mathrm{mod}}$, but it is the overall redistribution of the ion contributions that affects the $S_{\mathrm{A}}^{\mathrm{mod}}/S_{\mathrm{P}}^{\mathrm{mod}}$ relationship observed (figure 1). The overall effect of the redistribution of ions (table 3) on $S_{\mathrm{A}}^{\mathrm{mod}}$ and $S_{\mathrm{P}}^{\mathrm{mod}}$ was hence tested according to their modelled outputs at a normalised ionic strength of 0.72 mol $\mathrm{kg}_{\mathrm{H_2O}}^{-1}$ (figure 2). The trends at normalised ionic strength indicate that changes induced by

mirabilite precipitation between −6.4 and −22.8 °C display a lesser overall effect on $S_{\mathrm{A}}^{\mathrm{mod}}$ than $S_{\mathrm{P}}^{\mathrm{mod}}$, both increasing in salinity by 0.3 g $\mathrm{kg}_{\mathrm{sol}}^{-1}$ and 2.3, respectively.

It is important to note the absence of ikaite and gypsum from our experiments, both of which have been identified in natural and synthetic sea ice (Dieckmann et al., 2008; Geilfus et al., 2013; Fischer et al., 2013). Ikaite precipitation would not occur in the synthetic brines used for this investigation due to the absence of CO_3^{2-}, its precipitation from sea ice brines is understood to be a function of brine temperature and brine $p\mathrm{CO}_2$, the latter as an agent for the extent of ikaite saturation (Papadimitriou et al., 2013). The maximum total dissolved Ca^{2+} concentration change at brine-ikaite equilibrium has been measured to be 4 % during its precipitation in cryogenic brines to −7.5 °C (Papadimitriou et al., 2013). With respect to gypsum, the available scientific literature about its dynamics in sea ice contains inconsistent findings (Gitterman, 1937; Nelson and Thompson, 1954; Marion et al., 1999; Geilfus et al., 2013) and the potential extent of its precipitation from sea ice brines between −1.8 and −22.8 °C is largely undefined experimentally. The FREZCHEM code was therefore used to estimate the potential extent of gypsum precipitation in sea ice within this temperature range, and yielded maximum changes in total Ca^{2+} concentration of 10 %, with equimolar SO_4^{2-} removal.

Whilst it is currently difficult to know the true extent of ikaite and gypsum precipitation from sea ice brines, we used the higher estimates for their potential effects on brine composition to estimate the associated changes to $S_{\mathrm{A}}^{\mathrm{mod}}$ and S_{P}mod (using the same principles outlined in sections 2.3 and 2.4).

Table 3: The % contributions of the 6 constituent ions to $S_{\mathrm{A}}^{\mathrm{mod}}$ and $S_{\mathrm{P}}^{\mathrm{mod}}$ from conservative simplified seawater (DOE, 1994), to a sea ice brine at ice-brine-mirabilite equilibrium at −22.8 °C at 2 °C resolution.

T	$\%S_{\mathrm{A}}^{\mathrm{mod}}$						$\%S_{\mathrm{P}}^{\mathrm{mod}}$					
°C	Na^+	K^+	Mg^{2+}	Ca^{2+}	Cl^-	SO_4^{2-}	Na^+	K^+	Mg^{2+}	Ca^{2+}	Cl^-	SO_4^{2-}
Conserv.	30.754	1.138	3.662	1.184	55.525	7.737	26.435	1.091	6.317	1.291	61.394	3.472
−6.8	30.731	1.155	3.715	1.202	56.340	6.857	26.254	1.100	6.371	1.302	61.914	3.058
−8.8	30.663	1.203	3.869	1.252	58.673	4.341	25.746	1.126	6.520	1.333	63.372	1.903
−10.8	30.625	1.229	3.953	1.279	59.947	2.967	25.476	1.140	6.600	1.349	64.146	1.289
−12.8	30.603	1.245	4.004	1.295	60.719	2.134	25.315	1.148	6.648	1.359	64.609	0.922
−14.8	30.588	1.255	4.037	1.306	61.223	1.591	25.210	1.153	6.679	1.365	64.908	0.684
−16.8	30.578	1.262	4.060	1.313	61.569	1.218	25.139	1.157	6.699	1.369	65.112	0.523
−18.8	30.571	1.267	4.076	1.319	61.816	0.951	25.089	1.160	6.714	1.372	65.271	0.408
−20.8	30.565	1.271	4.083	1.322	61.998	0.755	25.052	1.162	6.725	1.375	65.364	0.323
−22.8	30.562	1.274	4.097	1.325	62.134	0.607	25.024	1.163	6.734	1.376	65.443	0.260

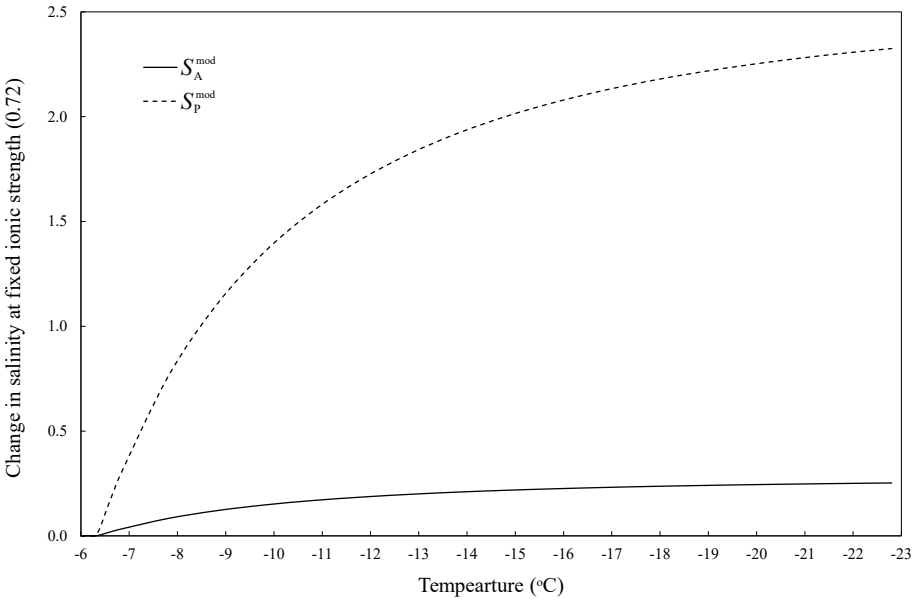

Figure 2: The change in $S_{\mathrm{A}}^{\mathrm{mod}}$ and $S_{\mathrm{P}}^{\mathrm{mod}}$ as a function of temperature, when the ionic strength of the brines are normalised by dilution to 0.72 mol $\mathrm{kg}_{\mathrm{H_2O}}^{-1}$.

Ikaite precipitation increased the difference between $S_{\mathrm{A}}^{\mathrm{mod}}$ and S_P^{mod} by up to 0.02 at -22.8 °C. Gypsum precipitation showed more notable effects, increasing the difference between $S_{\mathrm{A}}^{\mathrm{mod}}$ and $S_{\mathrm{P}}^{\mathrm{mod}}$ by up to 0.57 at -22.8 °C. Compared to the effects of mirabilite, which causes $S_{\mathrm{P}}^{\mathrm{mod}}$ to exceed $S_{\mathrm{A}}^{\mathrm{mod}}$ by 16.57 at -22.8°C, the potential contribution of ikaite and gypsum to the observed salinities presented here are relatively minimal. Nonetheless it is evident that ikaite and gypsum precipitation could further contribute to deviations between S_{P} and S_{A} in natural sea ice brines.

4. Discussion

4.1. The absolute salinity–temperature relationship in sea ice brines

Phase equations of sea ice, including the $S_A - T_{fr}$ relationship of sea ice brines at thermal equilibrium, are a common tool for estimating brine salinities when only temperature or bulk data is available (Cox and Weeks, 1986; Cox and Weeks, 1988; Garrison et al., 2003; Ewert and Deming, 2013; Collins et al., 2008). For this reason, accurate and up to date equations are a prerequisite for estimating the brine salinity reliably, and hence defining one of the key environmental constraints imposed upon sympagic biota.

The most comprehensive assessment to date of the $S_A - T_{fr}$ relationship of sea ice brines at thermal equilibrium is that of Assur (1960), who used major ion measurements (Na^+, K^+, Mg^{2+}, Ca^{2+}, Cl^- and SO_4^{2-}) in frozen seawater from Nelson and Thompson (1954), to deduce empirical equations from salt, water and ice mass balance. Assur (1960) used two discrete functions to describe the $S_A - T_{fr}$ relationship of sea ice brine, which converged at -8 °C, the temperature at which mirabilite precipitation was understood to initiate (Nelson and Thompson, 1954). Since 1960, Cox and Weeks (1986) and Notz and Worster (2009) have simplified the two original functions by fitting the same data to single polynomials for use in sea ice models (figure 3, top).

Our values of S_A^{mod} are derived from synthetic sea ice brines with a simplified ionic composition (table 1), which may introduce a slight bias compared to the more complex composition of natural seawater (table 1). Despite this, the ions included in the composition account for 99.4 % of the total S_A of Standard Seawater (Millero et al., 2008), and the 0.6 % difference is within the estimated error of S_A^{meas}. This reflects the accuracy of FREZCHEM in

describing Na^+ and SO_4^{2-} equilibria in sea ice brines as outlined in Butler et al. (2016). For these reasons, we use S_A^{mod} between −1.8 and −22.8 °C to refine the $S_A - T_{fr}$ relationship of sea ice brines, implicit of the most recent understanding of mirabilite precipitation (Marion et al., 1999; Butler et al., 2016), to be:

$$S_A(T_{fr}) = 2.2330 - 19.3188T_{fr} - 0.6574T_{fr}^2 - 0.0110T_{fr}^3 \quad (7)$$

$$T_{fr}(S_A) = -0.174808 - 0.044057S_A - 1.08933 \times 10^{-4}S_A^2 - 5.54349 \times 10^{-7}S_A^3, \quad (8)$$

where T_{fr} is the brine freezing point (°C) and S_A is in g kg_{sol}^{-1}. Regressions used to derive equations 7 and 8 (and equations hereafter) were computed using the Data Analysis Toolpak in Microsoft Excel, with error values (σ) representing the standard error of the fit ($S_A(T_{fr})$: $R^2 = 0.9998$, $\sigma = 0.807$, $n = 211$ $p < 0.001$; $T_{fr}(S_A)$: $R^2 = 0.99995$, $\sigma = 0.044$, $n = 211$, $p < 0.001$). We propose these equations for sea ice brines between −1.8 and −22.8 °C at brine-ice and brine-ice-mirabilite equilibrium. At −22.9 °C and below, hydrohalite precipitation results in further changes in brine composition and ionic ratios, and, therefore, an investigation of brine S_A and S_P below this temperature would require additional consideration of hydrohalite dynamics (Marion et al., 1999; Light et al., 2009; Butler and Kennedy, 2015).

Our refined $S_A - T_{fr}$ relationship generally corresponds well with the equations of Assur (1960), Cox and Weeks (1986), and Notz and Worster (2009) (figure 3, top). Major differences are seen around the temperature at which mirabilite begins to precipitate in sea ice, which recent investigation determined to occur at −6.4 °C (Butler et al., 2016) rather than the previously thought temperature of −8.2 °C (Nelson and Thompson, 1954; Assur, 1960).

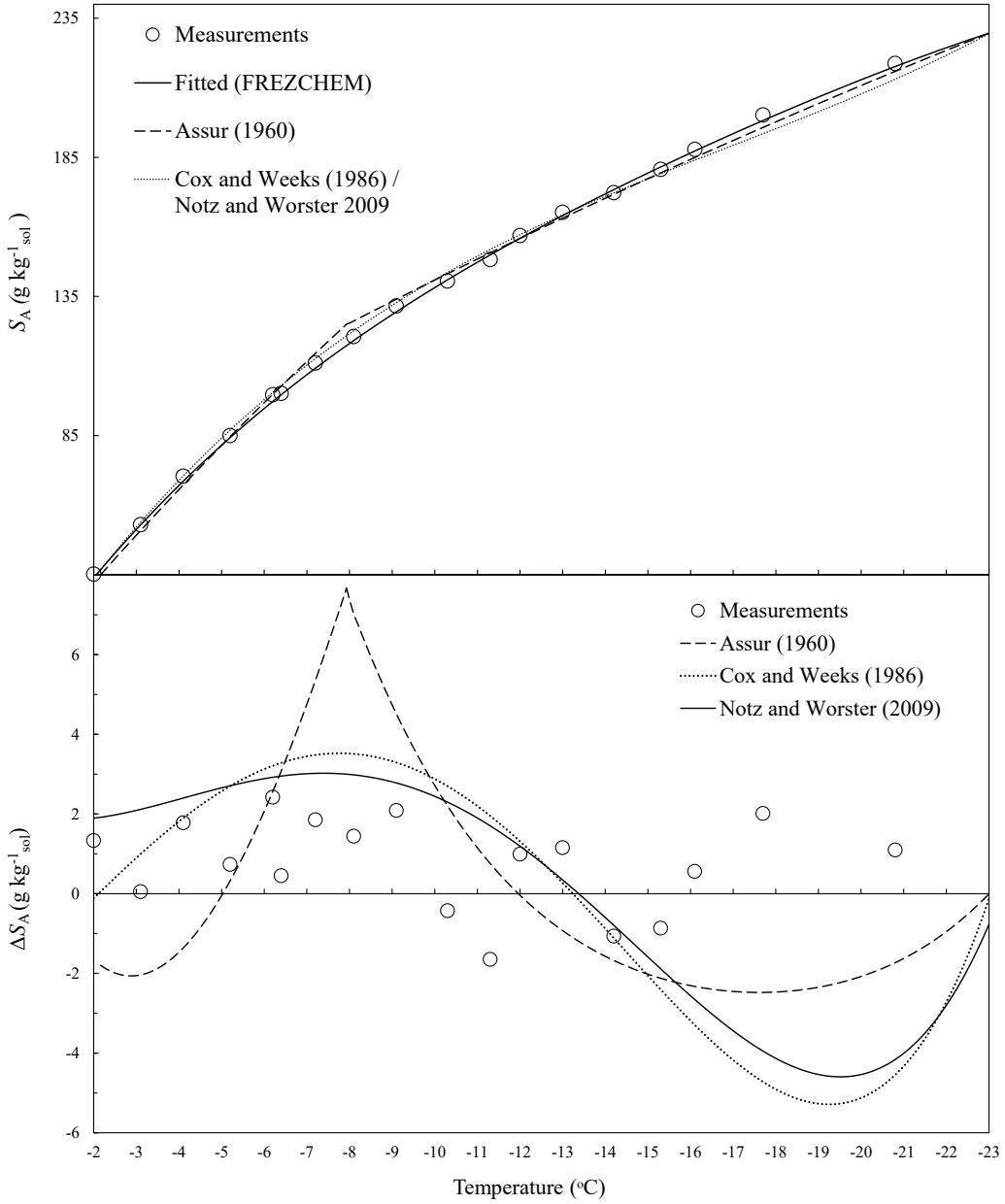

Figure 3: Top: A comparison of the refined $S_{\mathrm{A}} - T_{\mathrm{fr}}$ relationship (equation 7) with that of Assur (1960), Cox and Weeks (1986), and Notz and Worster (2009). Bottom: The ΔS_{A} of our measurements and other $S_{\mathrm{A}} - T_{\mathrm{fr}}$ equations, when compared to our refined $S_{\mathrm{A}} - T_{\mathrm{fr}}$ relationship of equation 7.

Further differences at approximately -19 °C, most notably with respect to the equations of Cox and Weeks (1986) and Notz and Worster (2009), are observed due to inaccuracies in fitting the Assur (1960) data to a single polynomial function. Compared to our refined $S_A - T_{fr}$ relationship of sea ice brines (equation 7), the previous equations over-estimate S_A by the greatest extent at -8 °C ($3.1 - 7.7$ g kg_{sol}^{-1}) and underestimate it by $2.5 - 5.3$ g kg_{sol}^{-1} below -17 °C (figure 3, bottom). The average error (ΔS_A) of our S_A^{meas} relative to equation 7 is 1.38 g kg_{sol}^{-1}, compared to ΔS_A of 3.10, 3.14 and 2.83 g kg_{sol}^{1} relative to the equations of Assur (1960), Cox and Weeks (1986), and Notz and Worster (2009), respectively.

The precipitation of ikaite and gypsum from sea ice brines could affect the accuracy of our refined $S_A - T_{fr}$ relationship. Using the highest available estimates for the extent of ikaite and gypsum precipitation outlined in section 3, the combined effect of their precipitation could decrease S_A by 0.02 g kg_{sol}^{-1} at -2 °C and 0.47 g kg_{sol}^{-1} at -22.8 °C. Compared to the changes induced by mirabilite precipitation, the potential effect of ikaite and gypsum is low. This analysis therefore indicates that incorporating up-to-date information about mirabilite dynamics (Butler et al., 2016) into the $S_A - T_{fr}$ relationship of equilibrium sea ice brines results in a more accurate description of brine salinities. The reduction in error compared to previous liquidus equations can be attributed to experimental and analytical limitations in the original investigation of Nelson and Thompson (1954), mainly relating to insufficient mirabilite equilibration in their experiments (Butler et al., 2016).

4.2. The practical salinity–temperature relationship in sea ice brines

Practical salinity is the property measured in sea ice field studies where it is almost exclusively assumed that $S_P = S_A$ (Gleitz et al., 1995; Krembs et al., 2000; Papadimitriou et al., 2004; Munro et al., 2010; Norman et al., 2011). This assumption is reasonable for brines that retain the ionic stoichiometry of Standard Seawater (table 1). However, it is now evident that the S_A/S_P of Standard Seawater is compromised in sea ice brines below -6.4 °C due to mirabilite precipitation. Our measured and modelled results indicate that S_P increases at a greater rate than S_A between -6.4 and -22.8 °C, approaching differences of >7 % as the temperature decreases (figures 1 and 2). This deviation substantiates the need for careful consideration of the S_A/S_P relationship in research involving sea ice brines with salinity measured on the practical scale as per typical field sampling protocols.

Existing state equations are related to S_A rather than S_P (section 4.1), which is not representative of the method by which sea ice brine salinity is currently measured in the field. Therefore, similarly to the $S_A - T_{fr}$ relationship for sea ice brines, an $S_P - T_{fr}$ relationship, implicit of mirabilite precipitation, can also be derived from this investigation. Owing to the accuracy of S_P^{mod} compared to our measurements (section 3), we fitted the modelled results between -1.8 and -22.8 °C first to an equation that yields S_P as a function of ice temperature T (°C) at ice-brine equilibrium:

$$S_P(T_{fr}) = 2.6105 - 18.8791T_{fr} - 0.5193T_{fr}^2 - 0.0070T_{fr}^3, \quad (9)$$

with $R^2 = 0.99998$, $\sigma = 0.295$, $n = 211$ and $p < 0.001$. Secondly, we derive an equation describing the brine freezing point (T_{fr}) as a function of S_P,

where

$$T_{\mathrm{fr}}(S_{\mathrm{P}}) = 0.3145 - 0.0605 S_{\mathrm{P}} + 3.1575 \times 10^{-5} S_{\mathrm{P}}^2 - 6.7696 \times 10^{-7} S_{\mathrm{P}}^3, \quad (10)$$

with $R^2 = 0.99999$, $\sigma = 0.016$, $n = 211$ and $p < 0.001$. Equation 10 can be used to accurately calculate the brine freezing point when only S_{P} data is available, which is typically the case for sea ice brines in field studies.

The $S_{\mathrm{P}} - T_{\mathrm{fr}}$ (equation 9) and $S_{\mathrm{A}} - T_{\mathrm{fr}}$ (equation 7) relationships are compared to available sea ice brine $S_{\mathrm{P}} - T_{\mathrm{fr}}$ data from the field (section 2.5) in figure 4. Between -2 and -6 °C, the field data follow our $S_{\mathrm{P}} - T_{\mathrm{fr}}$ and $S_{\mathrm{A}} - T_{\mathrm{fr}}$ relationships as would be expected while conservative physical concentration of seawater ions during freezing keeps the $S_{\mathrm{A}}/S_{\mathrm{P}}$ relationship constant and close to that of Standard Seawater. Below -7 °C the field brine S_{P} continues to increase at a greater rate than our $S_{\mathrm{A}} - T_{\mathrm{fr}}$ relationship, consistent with the divergence of S_{P} and S_{A} as a result of mirabilite-brine equilibrium. The field data are more accordant with our $S_{\mathrm{P}} - T_{\mathrm{fr}}$ relationship that is implicit of mirabilite precipitation but the field brine S_{P} increases at a slightly greater rate than our $S_{\mathrm{P}} - T_{\mathrm{fr}}$ relationship at temperatures below -9 °C. This difference may reflect the precipitation of other salts within the field brines (section 3) combined with their more complex solution composition. The discrepancies provide scope for further laboratory or field investigations with natural sea ice brines that may be able to account for these additional dynamics.

Norman et al. (2011) discuss that their measurements (figure 4), spanning from -1.3 to -12.4 °C ($n = 184$), evidently fit the empirical equation given

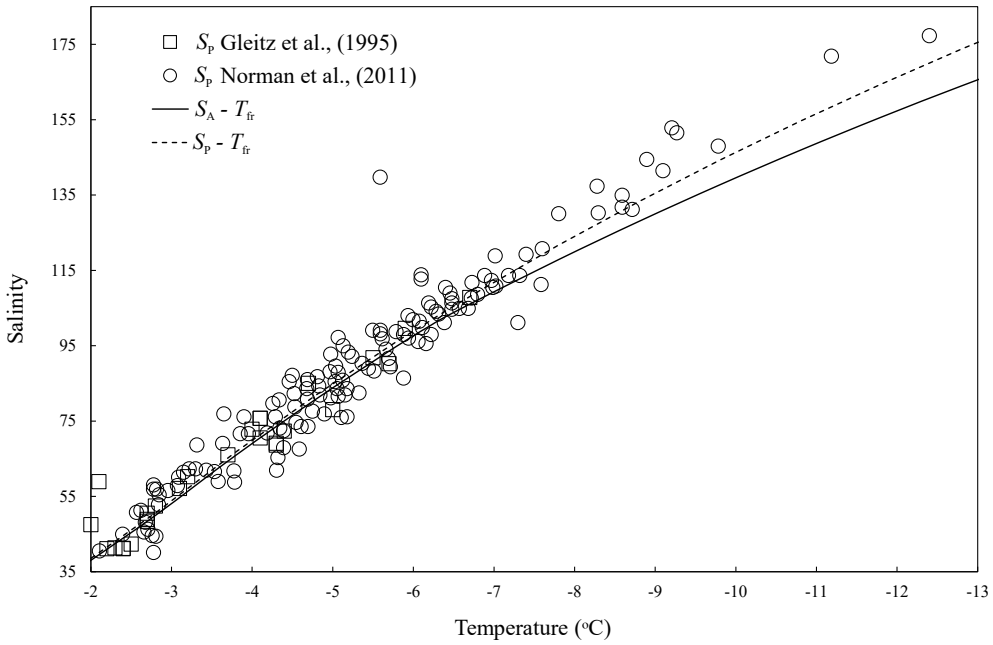

Figure 4: The S_{P} of natural sea ice brines, taken from Gleitz et al. (1995) and Norman et al. (2011), compared to our $S_{\mathrm{A}} - T_{\mathrm{fr}}$ (equation 7) and $S_{\mathrm{P}} - T_{\mathrm{fr}}$ (equation 9) relationships.

in Assur (1960),

$$S_{\mathrm{A}} = 1000 \left(1 - \frac{54.11}{T}\right)^{-1}, \tag{11}$$

which, as explicitly stated by Assur (1960), is only valid for use in sea ice brines down to -8 °C, prior to the onset of mirabilite precipitation. It would therefore not be expected for the field sea ice brine data to follow equation 11, unless the brine remained strongly supersaturated with respect to mirabilite, which is seemingly unlikely given its rapid change in solubility between -6 and -12 °C (Butler et al., 2016). Our data analysis instead indicates that the S_{P} measured in field sea ice brines obeys a similar $S_{\mathrm{P}} - T_{\mathrm{fr}}$ relationship to

that of equation 9 due to mirabilite precipitation and its consequent effect on brine composition. Whilst there are no measurements of S_A in natural sea ice brines that can be sourced for a direct comparison with the S_P measurements from the literature, all available data suggests that the universal assumption of an $S_A - S_P$ equivalence in sea ice brines is inaccurate in the region of mirabilite precipitation ($\leqslant -6.4$ °C).

The effect of using the easily measurable S_P instead of S_A for the calculation of brine density (ρ_b), brine volume fraction (v_b/v), brine freezing point, and the conversion factor (θ) between mol $kg^{-1}_{H_2O}$ and mol kg^{-1}_{sol} at -22.8 °C were evaluated here (table 4). All the differences (Δ) stem from the divergence of S_P from S_A displayed in figures 1 and 2, which deviate by 7.2 % at -22.8 °C. In relation to the sea ice properties, use of S_P results in a 13.26 kg m^{-3} overestimation of the brine density and an underestimation of brine volume fraction by 0.0027 (7.8 %). These differences, combined with a 3.15 °C underestimation of brine T_{fr} upon use of S_P highlight how any calculation of sea ice properties requires careful consideration of salinity, while the equivalence of S_A and S_P cannot be relied upon when dealing with non-conservative sea ice brines. Lastly, the use of S_P in calculation of θ, the concentration conversion factor, results in a 2.15 % underestimation of concentrations. Such differences could easily result in considerable inaccuracies when converting concentration units for use in thermodynamic models, such as FREZCHEM, or in models of ionic molal conductivities (McCleskey et al., 2012).

Table 4: The effect of using S_{P} rather than S_{A} (g $\mathrm{kg}_{\mathrm{sol}}^{-1}$) measurement upon the calculation of key physical sea ice parameters at −22.8 °C, with an idealised bulk sea ice S_{A} of 10 g $\mathrm{kg}_{\mathrm{sol}}^{-1}$.

	Brine	ρ_{b} [a]	$\frac{v_{\mathrm{b}}}{v}$ [b]	T_{fr} [c]	θ [d]
	Salinity	kg m^{-3}		°C	
S_{A}	229.71	1183.77	0.0314	−22.76	0.7703
S_{P}	246.28	1197.02	0.0341	−25.91	0.7537
$\Delta(S_{\mathrm{A}} - S_{\mathrm{P}})$	−16.57	−13.26	0.0027	3.15	0.0166
$\Delta S_{\mathrm{A}}(\%)$	−7.21	−1.12	7.7900	−13.84	2.1511

[a] $\rho_{\mathrm{b}} = 1000(1 + 0.0008 S_{\mathrm{A}})$ (Cox and Weeks, 1986)

[b] $\frac{v_{\mathrm{b}}}{v} = \frac{\rho_{\mathrm{si}} S_{\mathrm{si}}}{\rho_{\mathrm{b}} S_{\mathrm{A}}}$ (Cox and Weeks, 1983) where ρ_{si} is sea ice density (fixed at 0.926 g cm^{-3}) and S_{si} is the bulk sea ice salinity.

[c] Equation 7

[d] $\theta = 1 - 0.001 S_{\mathrm{A}}$ (Mucci, 1983)

4.3. Estimating absolute salinity from practical salinity

To facilitate a more accurate description of *in-situ* sea ice properties, we formulated a conversion factor (Φ), which may be used to estimate S_{A} from measurement of S_{P} in natural sea ice brines ($S_{\mathrm{P}}^{\mathrm{nat}}$) within the range of mirabilite precipitation. We assume that $S_{\mathrm{A}} = S_{\mathrm{P}}$ prior to mirabilite precipitation ($T > -6.4$ °C). For temperatures between −6.4 and −22.8 °C (brine S_{P} between 103 and 246), we derive Φ using $S_{\mathrm{P}}^{\mathrm{mod}}$ and $S_{\mathrm{A}}^{\mathrm{mod}}$. We

hence defined Φ as:

$$\Phi = \frac{S_{\mathrm{A}}^{\mathrm{mod}}}{S_{\mathrm{P}}^{\mathrm{mod}}}, \tag{12}$$

which was fitted to a third order polynomial function of $S_{\mathrm{P}}^{\mathrm{mod}}$ ($R^2 = 0.99997$, $\sigma = 0.0004$, $n = 165$, $p < 0.001$):

$$\Phi(S_{\mathrm{P}}) = 1.2090 - 3.4967 \times 10^{-3} S_{\mathrm{P}} + 1.538 \times 10^{-5} S_{\mathrm{P}}^2 - 2.333 \times 10^{-8} S_{\mathrm{P}}^3. \tag{13}$$

By calculating Φ from equation 13, the S_{P} of sea ice brines measured in the field ($S_{\mathrm{P}}^{\mathrm{nat}}$) may then be converted to an estimate of absolute salinity, $S_{\mathrm{A}}^{\mathrm{conv}}$, by

$$S_{\mathrm{A}}^{\mathrm{conv}} = S_{\mathrm{P}}^{\mathrm{nat}} \Phi. \tag{14}$$

Equation 13 was used to derive Φ for values of $S_{\mathrm{P}}^{\mathrm{nat}}$ ranging from 103 to 177 extracted from Norman et al. (2011), and hence estimate $S_{\mathrm{A}}^{\mathrm{conv}}$ (figure 5). The results show how Φ can aid in accounting for the effects of mirabilite precipitation on the salinity of sea ice brines, providing an estimate of S_{A}, whilst still exploiting the practical advantages of S_{P} measurement in the field. Use of Φ within this range approximately halved the average error of available data, relative to S_{A} (equation 7), from 6.81±5.36 %, to 3.49±4.15 %. Despite this improvement, Φ does not fully account for the difference between the measured S_{P} of natural brines in the field (figure 5) and the $S_{\mathrm{A}} - T_{\mathrm{fr}}$ relationship of equation 7. At present there are no measurements of sea ice brine S_{A} from the field, therefore current work is reliant upon the assumption that the brines are at thermal and chemical equilibrium. Additionally, the improved understanding of S_{A} and S_{P} in sea ice brines from this investigation cannot account for potential effects from the more complex composition of natural brines and the potential precipitation of ikaite and gypsum.

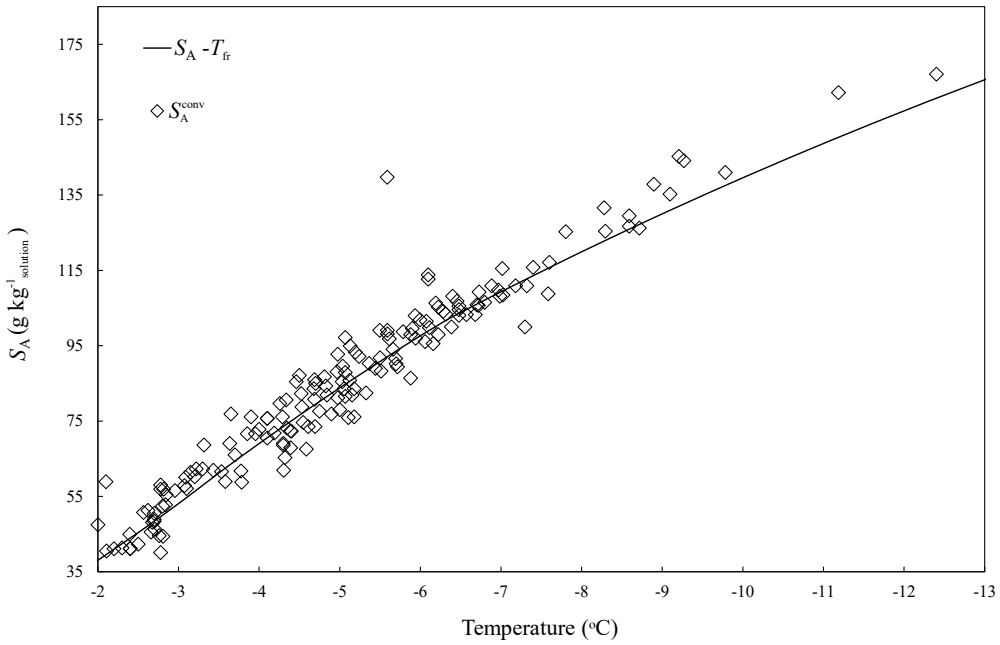

Figure 5: The $S_{\mathrm{A}}^{\mathrm{conv}}$ of natural sea ice brines versus brine temperature. The $S_{\mathrm{A}}^{\mathrm{conv}}$ was computed from S_{P} measurements in field samples of sackhole brines using equations 13 and 14. The field $S_{\mathrm{P}} - T_{\mathrm{fr}}$ data were taken from Gleitz et al. (1995) and Norman et al. (2011). The solid line represents the refined $S_{\mathrm{A}} - T_{\mathrm{fr}}$ equation of this study (equation 7).

4.4. The Density Salinity of sea ice brines

Methods of quantifying salinity are continuously developing in order to obtain the most accurate and reproducible measurements in aquatic environments. Since the introduction of PSS-78, the measurement of S_{P} has dominated oceanography at sea and in the laboratory. Here, it was shown that S_{P} is an unsuitable measure of salinity in sea ice brines when mirabilite precipitation causes non-conservative behaviour of Na^+ and SO_4^{2-}.

When PSS-78 was developed, conductivity was the conservative property of seawater that could be measured with the greatest accuracy and repro-

ducibility (Lewis, 1980). However, with recent advances in optical salinity sensors (Grosso et al., 2010), it is now also possible to measure the density of solutions very accurately, rapidly, and in an SI-traceable manner (IOC et al., 2010). Measurement of solution density can then be used to accurately determine S_A (Naftz et al., 2011). The most recent Thermodynamic Equation of Seawater 2010 (TEOS-10) computes S_A from the measurement of solution density, thus deriving 'Density Salinity' (S_A^{dens}) and decreasing the reliance upon conductivity-based salinity (IOC et al., 2010; Wright et al., 2011). The S_A^{dens} is the value of absolute salinity that is derived from the solution density at 25 °C and 0 dbar pressure. Whilst S_A^{dens} is defined for seawater in TEOS-10 (IOC et al., 2010), a similar protocol can be employed that is specific to sea ice brines, thus allowing S_A^{dens} determination from measurement of sea ice brine density.

The FREZCHEM code, shown to be accurate in the computation of S_A in sea ice brines, also computes brine density and hence can define the S_A^{dens} of this system. The accuracy of FREZCHEM for computing solution density can be shown from its output for Standard Seawater ($S_A = 35.157$ g kg_{sol}^{-1}) at 25 °C and 0 dbar pressure. FREZCHEM computes a density of 1023.356 kg m^{-3}, which is within 0.002 % of the value of 1023.334±0.0036 kg m^{-3} derived from the seawater density equation of Millero and Huang (2009). Following the IOC protocol, sea ice brine densities were computed by FREZCHEM at 25 °C and 0 dbar for the solution compositions that were used to calculate S_A^{mod} between −1.8 and −22.8 °C (section 2.3). From this, S_A^{dens} (g kg_{sol}^{-1}), which is equivalent to S_A^{mod}, can be described by a third order polynomial function of brine density ρ_b (kg m^{-3}) ($R^2 = 0.99999$, $\sigma = 0.176$, $p < 0.001$,

$n = 85$):

$$S_{\mathrm{A}}^{\mathrm{dens}} = 4.36370\times10^{3} - 14.59216\rho_{\mathrm{b}} + 1.48655\times10^{-2}\rho_{\mathrm{b}}^{2} - 4.63118\times10^{-6}\rho_{\mathrm{b}}^{3}. \quad (15)$$

The above $S_{\mathrm{A}}^{\mathrm{dens}} - \rho_{\mathrm{b}}$ relationship links this work to the current description of salinity in the TEOS-10 standards of practice. This approach is already employed for salinity measurements in hypersaline lakes (Naftz et al., 2011; Anati, 1999), hence the measurement of solution density at 25 °C rather than conductivity can be included in the sea ice standards of practice protocol as a reliable method for quantifying the salinity of sea ice brines. The assessment of S_{A} and S_{P} in this work offers a more comprehensive understanding of sea ice brine salinity, reliable means of determining it accurately, and guidelines for the improvement of field and laboratory measurements, all in line with current practice in oceanography. The caveat at present, however, is that the equations in this study are based on modelled synthetic brines with a simplified composition relative to that of brines in a natural sea ice system. Until measurements of natural brine S_{A} and density are made, the data and equations provided here for a simplified synthetic system remain the best available measure of sea ice brine salinities to −22.8 °C in the presence of mirabilite. For these reasons, future field work should include measurement of brine density and S_{A} along with the standard measurements of conductivity-based S_{P} to align the field of high latitude oceanic biogeochemistry with standard oceanographic practices (IOC et al., 2010).

5. Conclusions

Measurements and modelling of the ionic composition and electrical conductivity of synthetic sea ice brines between −1.8 and −22.8 °C have revealed

how mirabilite precipitation below −6.4 °C affects the S_A and S_P of the brine to a measurable, and different, extent for each parameter. We have first refined the $S_A - T_{fr}$ relationship for sea ice brines to account for the new and comprehensive information about mirabilite precipitation in sea ice brines. Furthermore, the first $S_P - T_{fr}$ relationship has been formulated for sea ice brines at thermal equilibrium. Our analysis has shown that, between −6.4 and −22.8 °C, the S_P increases at a greater rate than S_A due to the redistribution of individual ion contributions to the total electrical conductivity of the solution and the total concentration of dissolved salts. As a result, it is highlighted that the widespread assumption of S_A and S_P equivalence in sea ice brines incurs and propagates errors in the calculation of key physical parameters of the sea ice system, whilst misrepresenting the conditions inhabited by sympagic organisms. Existing data of field sea ice brine S_P from the Southern Ocean is in agreement with our modelled and measured data from synthetic seawater brines. We therefore propose that the observed $S_P - T_{fr}$ relationship in natural sea ice brines is a reflection of mirabilite precipitation in the field temperature region where this reaction is expected to occur ($T \leqslant -6.4$ °C). The ease with which electrical conductivity can be measured for S_P determination will likely cement its use in field investigations for years to come. We have therefore formulated a conversion factor for estimation of S_A from measurement of S_P in sea ice brines affected by mirabilite precipitation. To help progress towards a description of sea ice brine salinity that is aligned with the most recent oceanography standard, TEOS-10, we have also formulated a relationship between absolute salinity and brine density.

The equations maintain the current paradigm that brines attain thermal and chemical equilibrium, and could be further refined with additional investigations using naturally derived seawater brines. Similar work in the coldest temperature region of sea ice, between -23 °C and the eutectic, where other minerals are understood to precipitate and interact, could aid in developing an accurate understanding of salinity in such hypersaline and non-conservative conditions.

6. Acknowledgements

The work was supported by a NERC Algorithm Studentship (NE/K501013), beamtime awards EE-3897-1 and EE-12301-1 from Diamond Light Source Ltd, and a PhD Student Grant from the International Association of Geochemistry. We are very thankful to the I11 beamline team, Professor Chiu Tang, Dr Sarah Day and Dr Claire Murray for their support during beamtime. The generosity of advice and resources from Dr Vera Thoss in the School of Chemistry, Bangor University, was invaluable throughout this investigation. We also thank the three anonymous reviewers for their constructive comments, which helped to improve this paper. All data presented here are freely available upon contacting the corresponding author.

References

Anati, D. A., 1999. The salinity of hypersaline brines: concepts and misconceptions. International Journal of Salt Lake Research 8 (1), 55–70.

Assur, A., 1960. Composition of sea ice and its tensile strength. Tech. rep.,

620 44, Arctic Sea Ice, U.S. National Academy of Sciences, National Research
621 Council, U.S.A.

622 Butler, B. M., Kennedy, H., 2015. An investigation of mineral dynamics in
623 frozen seawater brines by direct measurement with synchrotron X-ray pow-
624 der diffraction. Journal of Geophysical Research: Oceans 120 (8), 5686–
625 5697.

626 Butler, B. M., Papadimitriou, S., Santoro, A., Kennedy, H., 2016. Mirabilite
627 solubility in equilibrium sea ice brines. Geochimica et Cosmochimica Acta
628 182, 40 – 54.

629 Collins, R. E., Carpenter, S. D., Deming, J. W., 2008. Spatial heterogeneity
630 and temporal dynamics of particles, bacteria, and pEPS in Arctic winter
631 sea ice. Journal of Marine Systems 74 (3), 902–917.

632 Cox, G. F. N., Weeks, W. F., 1983. Equations for determining the gas and
633 brine volumes in sea ice samples. Journal of Glaciology 29 (102), 306–316.

634 Cox, G. F. N., Weeks, W. F., 1986. Changes in the salinity and porosity
635 of sea-ice samples during shipping and storage. Journal of Glaciology 32,
636 371–375.

637 Cox, G. F. N., Weeks, W. F., 1988. Numerical simulations of the profile prop-
638 erties of undeformed first-year sea ice during the growth season. Journal
639 of Geophysical Research: Oceans 93 (C10), 12449–12460.

640 Dieckmann, G. S., Hellmer, H. H., 2010. The importance of sea ice: An
641 overview. Sea Ice 2, 1–22.

642 Dieckmann, G. S., Nehrke, G., Papadimitriou, S., Göttlicher, J., Steininger,
643 R., Kennedy, H., Wolf-Gladrow, D., Thomas, D. N., 2008. Calcium car-
644 bonate as ikaite crystals in Antarctic sea ice. Geophysical Research Letters
645 35 (8), L08501.

646 Dittmar, W., Thomson, C., Buchanan, J., 1873. Report on Researches Into
647 the Composition of Ocean-Water. Report on the scientific results of the
648 voyage of H.M.S. Challenger during the years 1873-1876. Physics and chem-
649 istry.

650 DOE, 1994. Handbook of methods for the analysis of the various parameters
651 of the carbon dioxide system in sea water; version 2. A. G. Dickson & C.
652 Goyet ORNL/CDIAC.

653 Ewert, M., Deming, J. W., 2013. Sea ice microorganisms: Environmental
654 constraints and extracellular responses. Biology 2 (2), 603–628.

655 Fischer, M., Thomas, D. N., Krell, A., Nehrke, G., Göttlicher, J., Norman, L.,
656 Meiners, K. M., Riaux-Gobin, C., Dieckmann, G. S., 2013. Quantification
657 of ikaite in Antarctic sea ice. Antarct. Sci 25 (3), 421–432.

658 Fofonoff, N., 1985. Physical properties of seawater: A new salinity scale and
659 equation of state for seawater. Journal of Geophysical Research: Oceans
660 (1978–2012) 90 (C2), 3332–3342.

661 Forchhammer, G., 1865. On the composition of sea-water in the different
662 parts of the ocean. Philosophical Transactions of the Royal Society of Lon-
663 don 155, 203–262.

664 Garrison, D. L., Jeffries, M. O., Gibson, A., Coale, S. L., Neenan, D., Fritsen,
665 C., Okolodkov, Y. B., Gowing, M. M., 2003. Development of sea ice mi-
666 crobial communities during autumn ice formation in the Ross Sea. Marine
667 Ecology Progress Series 259, 1–15.

668 Geilfus, N.-X., Galley, R. J., Cooper, M., Halden, N., Hare, A., Wang, F.,
669 Søgaard, D. H., Rysgaard, S., 2013. Gypsum crystals observed in experi-
670 mental and natural sea ice. Geophysical Research Letters 40 (24), 6362–
671 6367.

672 Gitterman, K. E., 1937. Thermal analysis of seawater. Tech. rep., CRREL
673 TL287, USA Cold Region Research and Engineering Laboratory, Hanover,
674 N.H.

675 Gleitz, M., vd Loeff, M. R., Thomas, D. N., Dieckmann, G. S., Millero,
676 F. J., 1995. Comparison of summer and winter inorganic carbon, oxygen
677 and nutrient concentrations in Antarctic sea ice brine. Marine Chemistry
678 51 (2), 81–91.

679 Golden, K. M., Eicken, H., Heaton, A. L., Miner, J., Pringle, D. J., Zhu,
680 J., 2007. Thermal evolution of permeability and microstructure in sea ice.
681 Geophysical Research Letters 34, L16501.

682 Grasby, S. E., Rod Smith, I., Bell, T., Forbes, D. L., 2013. Cryogenic forma-
683 tion of brine and sedimentary mirabilite in submergent coastal lake basins,
684 Canadian Arctic. Geochimica et Cosmochimica Acta 110, 13–28.

685 Grosso, P., Le Menn, M., De La, J.-L. D. B., Wu, Z. Y., Malardé, D.,
686 et al., 2010. Practical versus absolute salinity measurements: New ad-

vances in high performance seawater salinity sensors. Deep Sea Research Part I: Oceanographic Research Papers 57 (1), 151–156.

He, S., Morse, J. W., 1993. The carbonic acid system and calcite solubility in aqueous Na-K-Ca-Mg-Cl-SO_4 solutions from 0 to 90 °C. Geochimica et Cosmochimica Acta 57 (15), 3533–3554.

Horner, R., Ackley, S. F., Dieckmann, G. S., Gulliksen, B., Hoshiai, T., Legendre, L., Melnikov, I. A., Reeburgh, W. S., Spindler, M., Sullivan, C. W., 1992. Ecology of sea ice biota. Polar Biology 12 (3-4), 417–427.

Howarth, R. W., 1978. A rapid and precise method for determining sulfate in seawater, estuarine waters, and sediment pore waters. Limnology and Oceanography 23 (5), 1066–1069.

IOC, SCOR, IAPSO, 2010. The international thermodynamic equation of seawater–2010: Calculation and use of thermodynamic properties. Tech. rep., Intergovernmental Oceanographic Commission, Manuals and Guides No. 56 (UNESCO).

Jackett, D. R., McDougall, T. J., Feistel, R., Wright, D. G., Griffies, S. M., 2006. Algorithms for density, potential temperature, conservative temperature, and the freezing temperature of seawater. Journal of Atmospheric and Oceanic Technology 23 (12), 1709–1728.

Kester, D. R., Duedall, I. W., Connors, D. N., Pytkowicz, R. M., 1967. Preparation of artifical seawater. Limnology and Oceanography 12 (1), 176–179.

709 King, B. A., Firing, E., Joyce, T. M., 2001. Ocean Circulation and Climate:
710 Observing and Modelling the Global Ocean. International geophysics se-
711 ries. Academic Press, San Fransisco CA, USA, Ch. Shipboard observations
712 during WOCE.

713 Krembs, C., Gradinger, R., Spindler, M., 2000. Implications of brine chan-
714 nel geometry and surface area for the interaction of sympagic organisms
715 in Arctic sea ice. Journal of Experimental Marine Biology and Ecology
716 243 (1), 55–80.

717 Lewis, E., 1980. The practical salinity scale 1978 and its antecedents. IEEE
718 Journal of Oceanic Engineering 5 (1), 3–8.

719 Light, B., Brandt, R. E., Warren, S. G., 2009. Hydrohalite in cold sea ice:
720 Laboratory observations of single crystals, surface accumulations, and mi-
721 gration rates under a temperature gradient, with application to Snowball
722 Earth. Journal of Geophysical Research 114 (C7), C07018.

723 Light, B., Maykut, G. A., Grenfell, T. C., 2003. Effects of temperature on the
724 microstructure of first-year Arctic sea ice. Journal of Geophysical Research
725 108 (C2), 3051.

726 Marion, G. M., Farren, R. E., Komrowski, A. J., 1999. Alternative pathways
727 for seawater freezing. Cold Regions Science and Technology 29, 259–266.

728 Marion, G. M., Kargel, J. S., 2008. Cold Aqueous Planetary Geochemistry
729 with FREZCHEM. Springer, Heidelberg.

730 Marion, G. M., Mironenko, M. V., Roberts, M. W., 2010. FREZCHEM: A

731 geochemical model for cold aqueous solutions. Computers & Geosciences
732 36, 10–15.

733 McCaffrey, M., Lazar, B., Holland, H., 1987. The evaporation path of sea-
734 water and the coprecipitation of Br^- and K^+ with halite. Journal of Sedi-
735 mentary Research 57 (5), 928–937.

736 McCleskey, R. B., Nordstrom, D. K., Ryan, J. N., Ball, J. W., 2012. A new
737 method of calculating electrical conductivity with applications to natural
738 waters. Geochimica et Cosmochimica Acta 77, 369 – 382.

739 Miller, L. A., Papakyriakou, T. N., Collins, R. E., Deming, J. W., Ehn, J. K.,
740 Macdonald, R. W., Mucci, A., Owens, O., Raudsepp, M., Sutherland, N.,
741 2011. Carbon dynamics in sea ice: A winter flux time series. Journal of
742 Geophysical Research: Oceans 116 (C2), c02028.

743 Millero, F. J., Feistel, R., Wright, D. G., McDougall, T. J., 2008. The
744 composition of Standard Seawater and the definition of the Reference-
745 Composition Salinity Scale. Deep Sea Research Part I 55, 50–72.

746 Millero, F. J., Huang, F., 2009. The density of seawater as a function of
747 salinity (5 to 70 g kg^{-1}) and temperature (273.15 to 363.15 K). Ocean
748 Science 5 (2), 91–100.

749 Millero, F. J., Leung, W. H., 1976. The thermodynamics of seawater at one
750 atmosphere. American Journal of Science 276 (9), 1035–1077.

751 Mucci, A., 1983. The solubility of calcite and aragonite in seawater at vari-
752 ous salinities, temperatures, and one atmosphere total pressure. American
753 Journal of Science 283, 780–799.

Munro, D. R., Dunbar, R. B., Mucciarone, D. A., Arrigo, K. R., Long, M. C., 2010. Stable isotope composition of dissolved inorganic carbon and particulate organic carbon in sea ice from the Ross Sea, Antarctica. Journal of Geophysical Research: Oceans 115 (C9), c09005.

Naftz, D. L., Millero, F. J., Jones, B. F., Green, W. R., 2011. An equation of state for hypersaline water in Great Salt Lake, Utah, USA. Aquatic geochemistry 17 (6), 809–820.

Nelson, K. H., Thompson, T. G., 1954. Deposition of salts from sea water by frigid concentration. Tech. rep., 29, Office of Naval Research, Arlington, VA.

Norman, L., Thomas, D. N., Stedmon, C. A., Granskog, M. A., Papadimitriou, S., Krapp, R. H., Meiners, K. M., Lannuzel, D., van der Merwe, P., Dieckmann, G. S., 2011. The characteristics of dissolved organic matter (DOM) and chromophoric dissolved organic matter (CDOM) in Antarctic sea ice. Deep Sea Research Part II: Topical Studies in Oceanography 58 (910), 1075 – 1091.

Notz, D., Worster, M. G., May 2009. Desalination processes of sea ice revisited. Journal of Geophysical Research 114, C05006.

Papadimitriou, S., Kennedy, H., Kattner, G., Dieckmann, G., Thomas, D., 2004. Experimental evidence for carbonate precipitation and CO_2 degassing during sea ice formation. Geochimica et Cosmochimica Acta 68 (8), 1749–1761.

776 Papadimitriou, S., Kennedy, H., Kennedy, P., Thomas, D. N., 2013. Ikaite
777 solubility in seawater-derived brines at 1 atm and sub-zero temperatures
778 to 265 K. Geochimica et Cosmochimica Acta 109, 241–253.

779 Papadimitriou, S., Thomas, D. N., Kennedy, H., Haas, C., Kuosa, H., Krell,
780 A., Dieckmann, G. S., 2007. Biogeochemical composition of natural sea ice
781 brines from the Weddell Sea during early austral summer. Limnology and
782 Oceanography 52 (5), 1809–1823.

783 Pawlowicz, R., 2012. The electrical conductivity of seawater at high temper-
784 atures and salinities. Desalination 300, 32 – 39.

785 Pawlowicz, R., 2015. The absolute salinity of seawater diluted by riverwater.
786 Deep Sea Research Part I: Oceanographic Research Papers 101, 71 – 79.

787 Perkin, R. G., Lewis, E. L., 1980. The practical salinity scale 1978: fitting
788 the data. Oceanic Engineering 5 (1), 9–16.

789 Petrich, C., Eicken, H., 2010. Growth, structure and properties of sea ice.
790 Sea Ice 2, 23–77.

791 Pitzer, K. S., 1973. Thermodynamics of electrolytes. I. Theoretical basis and
792 general equations. The Journal of Physical Chemistry 77 (2), 268–277.

793 Thomas, D. N., Dieckmann, G. S., 2002. Antarctic Sea ice-a habitat for
794 extremophiles. Science 295, 641–644.

795 Thomas, D. N., Papadimitriou, S., Michel, C., 2010. Biogeochemistry of sea
796 ice. Sea Ice 2, 425–467.

797 Weeks, W., 2010. On Sea Ice. University of Alaska Press.

798 Weeks, W. F., Ackley, S. F., 1986. The growth, structure, and properties of
799 sea ice. Springer.

800 Wright, D., Pawlowicz, R., McDougall, T., Feistel, R., Marion, G., 2011.
801 Absolute salinity,"density salinity"and the reference-composition salinity
802 scale: present and future use in the seawater standard teos-10. Ocean
803 Science 7 (1), 1–26.